Phase Changes and Electronic Properties in Toroidal Mesoporous Molybdenum Oxides**

David M. Antonelli* and Michel Trudeau

Highly ordered porous transition metal oxides are predicted to be useful in a wide variety of areas where flexible redox activity and unique magnetic and electronic properties are necessary. Such areas include the synthesis of quantum wires and nanomagnetic devices, the design of hydrogen storage materials for batteries, the development of new catalysts for oxidation of organic substrates, and the fabrication of wave guides, membranes, and sensor components. By manipulating synthesis conditions it is possible to control the porosity of metal oxides on both the nanometer[1–3] and the micron level.[4, 5] Hexagonally packed mesoporous silicas can be synthesized with a wide variety of shapes including toroid and discoid morphologies,[6–8] demonstrating that not only can the meso- and macroscopic porosity of a material be controlled, but the overall shape and macroscopic design of the oxide array can be manipulated to synthesize materials with order on several levels of scale. Herein we describe the synthesis of semiconducting mesostructured mixed oxidation state molybdenum bronzes which selectively form toroid shapes with diameters of several hundred nanometers.

While d^0 mesoporous transition metal oxides of Nb,[3, 9] Ta,[10] Zr,[11–13] Ti,[14] and Hf[15] have been synthesized, there are few examples of mesoporous oxides of metals with partially filled d shells. The presence of unpaired electrons in the walls of the mesostructure should lead to unusual magnetic and electronic properties not displayed by their d^0 counterparts. Mixed oxidation state mesoporous Mn oxides were recently synthesized by a liquid crystal templating strategy.[8] This material was the first conducting mesoporous oxide. In order to exploit the inherent magnetic properties of unpaired electrons in metal oxide materials we aimed at synthesizing a d^1 mesoporous Mo^V oxide. It is known that self-assembly of W^{VI} and Mo^{VI} oxides in the presence of cationic surfactants leads to the formation of hexagonally packed surfactant salts of W and Mo oxo clusters which were not stable to surfactant removal.[16] Mesoporous niobium and tantalum oxides can be synthesized by ligation of amine templates to $M(OEt)_5$ (M = Nb, Ta) followed by hydrolysis and template removal by acid treatment. By analogy, $Mo(OEt)_5$ was combined with dodecylamine in varying concentrations and subsequently hydrolyzed. Under these conditions only amorphous materials were formed. Under the assumption that the lower Lewis acidity of the d^1 Mo center as compared to the d^0 Nb center was retarding dodecylamine binding, we synthesized a dimeric molybdenum ethoxide complex (Scheme 1) with a bridging dodecylimido group, thus establishing the required surfactant–metal interaction prior to hydrolysis. The stoichiometry of this complex ensured that the 2:1 metal to surfactant ratio, optimal for Nb-TMS1 formation, was maintained. Addition of water to solutions of this complex in ethanol at pH values ranging from 3–7 led to formation of foamy brown solutions which yielded bronze mesostructured Mo oxide (Mo-TMS1) after aging at 90 °C for two weeks. The X-ray powder diffraction (XRD) pattern (Figure 1A) shows a high-intensity (100) peak at $d = 32$ Å and less resolved lower angle peaks,

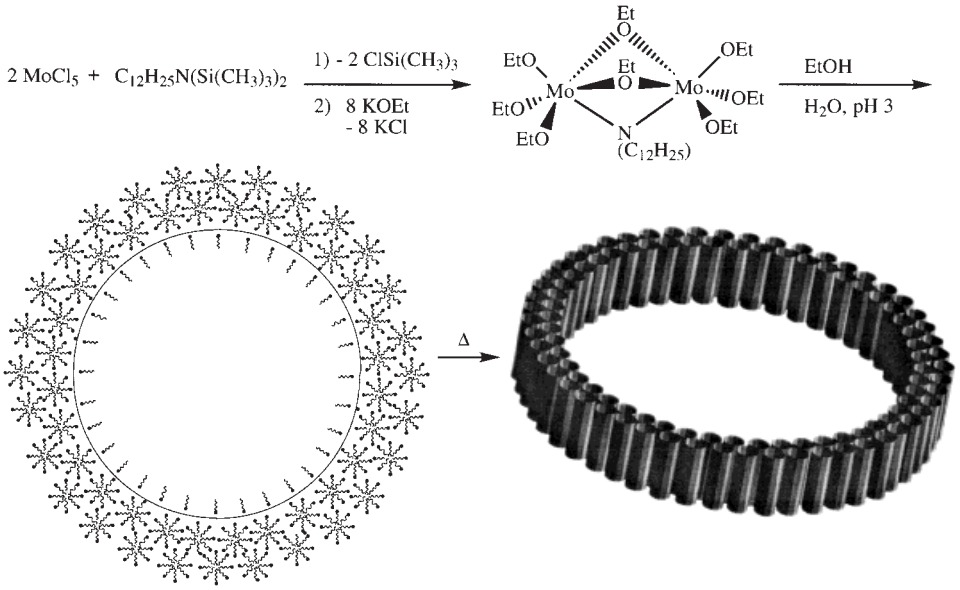

Scheme 1. Synthetic scheme for formation of mesostructured molybdenum oxide (Mo-TMS1) toroids. Treatment of molybdenum pentachloride with bis(trimethylsilyl)dodecylamine in dichloromethane led to the formation of a molybdenum imido chloride complex, the dimeric structure of which was assigned on the basis of analogous imido complexes previously synthesized. Reaction of this complex with potassium ethoxide in toluene led to the formation of a viscous brown oil formulated as the imido octaethoxy dimer (shown top right). Dissolution of this complex in ethanol followed by treatment of the resulting brown solution with water at pH 3 gave a foamy brown solution. Heating this solution for two weeks at 90 °C gave toroidal Mo-TMS1. The formation of toroids is rationalized on the basis of microphase separation through microbubble (as shown in the center) or vessicle formation which templates the crystallization of micellar molybdenum oxide/surfactant aggregates. In this strategy the dodecylamine acts as a two-way templating agent, directing formation of both the micelles and the spherical macrostructure (shown schematically bottom right).

[*] Dr. D. Antonelli
Department of Chemistry and Biochemistry
University of Windsor
Windsor ON (Canada)
Fax: (+1) 519 973-7098
E-mail: danton@server.uwindsor.ca
Dr. M. Trudeau
Emerging Technologies, Hydro-Québec Research Institute
1800 Boul. Lionel-Boulet, Varennes, Québec, J3X 1S1 (Canada)

[**] We thank Julian Thorpe at The University of Sussex for his assistance in electron microscopy and The Royal Society for financial support.

  1433-7851/99/3810-1471 $ 17.50+.50/0

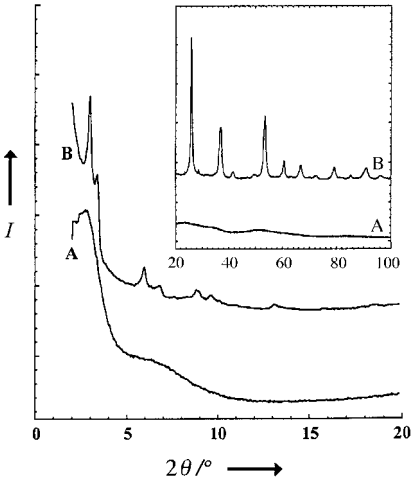

Figure 1. XRD patterns of as-synthesized a) hexagonal bronze and b) lamellar blue mesostructured molybdenum oxide obtained on a Siemens D500 θ-2θ diffractometer with $Cu_{K\alpha}$ radiation ($\lambda = 1.5418$ Å). The phase change from the molybdenum bronze to the molybdenum blue is accompanied by the appearance of higher angle peaks as shown in the inset.

which confirm the mesostructured nature of this material. The high-angle diffraction pattern (insert) does not show any structure. This is indicative of the amorphous nature of the wall structure. The broadened reflections as compared to those of MCM-41 are typical of materials synthesized with neutral templates,[17] and suggest a lower degree of mesoscopic order than those materials synthesized with charged surfactants. When ethanol was not added to the synthesis mixture or the hydrolysis was conducted at pH values less than 1, lamellar materials were formed. The elemental analysis of the hexagonal Mo-TMS1 gave values of C 19.83, H 4.04, and N 1.71%, demonstrating that the surfactant had been retained in the structure. Figure 2 presents the X-ray photoelectron spectra (XPS) for the air-exposed surface of the powder taken using monochromatic $Al_{K\alpha}$ radiation. The peak

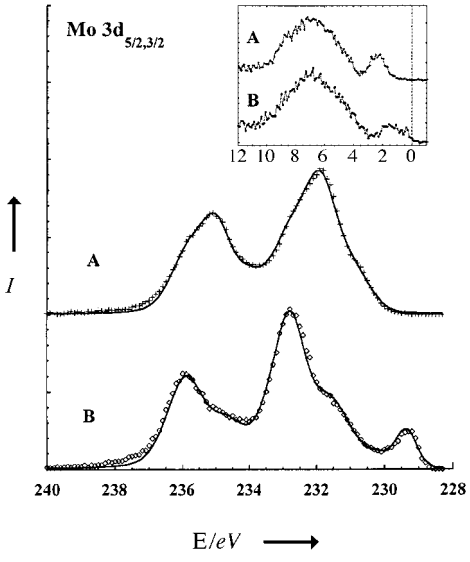

Figure 2. XPS 3d emission for the two Mo samples (A = bronze, B = blue) with an inset showing their corresponding valence spectra. The dashed line in this inset represents the Fermi level. The valence spectra values suggest that the bronze is semiconducting and the blue is metallic.

positions were referenced to the C-(C,H) carbon emission at 284.8 eV. Peak deconvolution revealed that the $3d_{5/2}$ emission is composed of three contributions: a major one at 231.9 eV and two smaller ones at 232.8 and 230.9 eV. Based on reference tables[18] this would indicate that the molybdenum at the surface would be present mostly in the +6 state, indicating that a small degree of surface air oxidation has taken place during the synthesis procedure. On the other hand, the measured surface Mo:O ratio was found to be about 51%, after removing the O atoms present in C–O groups, which would agree with the formation of MoO_2. It should be mentioned that an emission at 232 eV has previously been attributed to MoO_2.[19] Ozin et al. report that 1 eV can be added for each increase in oxidation state from Mo metal (228 eV),[20] and thus the peaks at 232–233 eV could also be due to Mo^V. The inset in Figure 2 presents the valence spectra for the bronze mesostructure and shows the semiconducting nature of the bronze mesostructure with a gap of about 1.3 eV to the Fermi level. This indicates that this material is a semiconductor, which may have numerous applications in the nanofabrication of materials with unique electronic properties. Conductivity measurements of this material gave a value of $2.5 \times 10^{-12}\ \Omega\,cm^{-1}$, which is extremely low on the basis of the XPS data and can be explained by the discontinuous nature and low density of the Mo bronze which can lead to experimental densification and resistivity measurement problems. This was confirmed by the UV/Vis reflectance mode spectrum[21] of this material which displayed an absorbance at 330 nm corresponding to a band gap of 3.75 eV. This is very similar to the value of 3.18 eV observed for mesoporous Mn oxide.

Low magnification transmission electron microscope (TEM) images of samples of Mo-TMS1 prepared by laying thin microtomed sections over carbon-coated grids revealed a fascinating array of ringlike structures (Figure 3a) approximately 300 nm in diameter. Some of the rings had smaller rings inside them, forming unique living cell-like structures. Although most of these structures were free-standing rings, some had fused together to form random structures similar to those observed for mesolamellar aluminophosphates.[22, 23] This contrasts with emulsion-templated macroporous Ti, Zr, and Si oxide-based materials,[5] which form sheets with long-range hexagonal packing of the individual macropores but have no well-ordered porous patterns on the mesoscopic level. Higher magnification of the toroidal face in samples of Mo-TMS1 revealed that these structures were constructed of mesotubules of roughly 50 nm in length and 3 nm in diameter (Figure 3b). This value is consistent with the position of the (100) peak at 32 Å in the XRD pattern. Unusually, clusters of smaller toroids reorder into larger toroids over a matter of seconds under the influence of a TEM electron beam. Energy dispersive X-ray spectroscopy (EDS) showed that this material was rich in molybdenum, confirming that the ringlets were indeed composed of mesostructured molybdenum oxide. Previous work has shown that toroidal mesoporous silicate forms can be generated by manipulation of the synthesis conditions to favor curvature in propagating silica–surfactant micelles.[7] The mesotubes in these silica-based toroids run along the plane of the ringlets and not perpendicular to the

  1433-7851/99/3810-1472 $ 17.50+.50/0

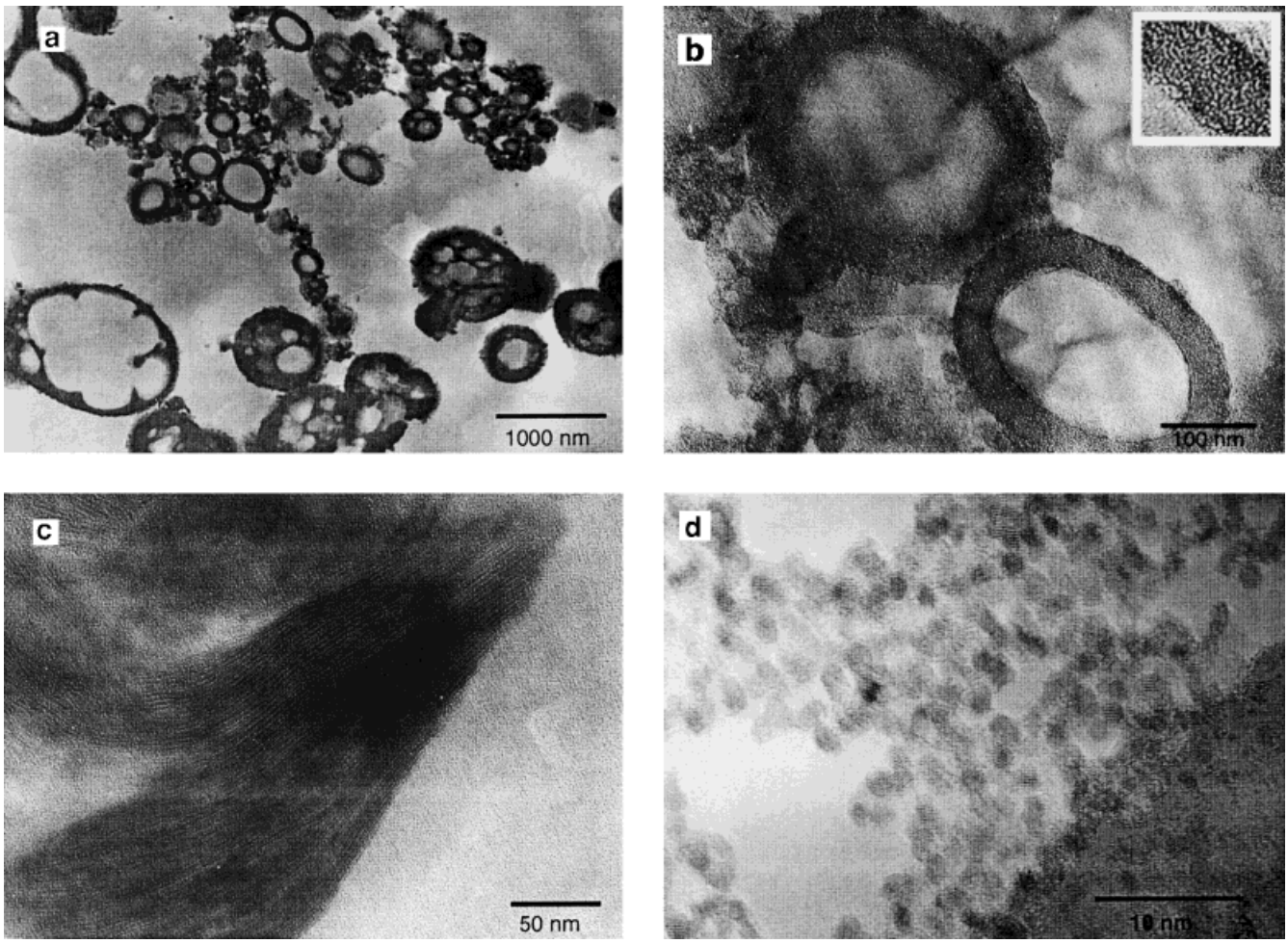

Figure 3. TEM images of molybdenum oxide bronzes: a) at low magnification revealing the toroidal structures (see text for details); b) at higher magnification. The further-magnified inset reveals the mesostructured nature of the walls of the toroid. Scanning electron microscopy (SEM) revealed no salient structural features or tubular forms, indicating that these toroids are relatively flat (ca. 50 nm). Other areas of sample exist in which there is no higher order to the mesostructured system, although the toroidal regions dominate the material; c) lamellar region of the mesostructured molybdenum oxide blue showing that certain regions of the bronze have reordered into a layered phase in the blue; d) close up of a region of the molybdenum blue showing where crystallization of the walls of the mesostructure into oxide grains about 1.5 nm in size has led to partial degradation of the occluded mesopores. Samples were prepared either by sonication in isopropyl alcohol or microtoming followed by deposition on a carbon-coated copper grid. Micrographs were recorded at 300 KV on a Hitachi H-9000 STEM.

plane as observed for the molybdenum bronze toroids. This suggests a mechanism in which the surfactant acts as a twofold templating agent, not only directing the formation of the individual mesotubes, but also forming either vesicles or microbubbles or by microphase separation which template the crystallization of the tubules into highly ordered ring structures (Scheme 1). This mechanism is likely related to that proposed for diatomaceous mesolamellar aluminophosphates,[22, 23] with the exception that ordered pores rather than layers are formed on the mesoscopic level. The factors governing formation of these toroids were studied and it was found that the presence of KCl in the synthesis mixture clearly promotes toroid formation, as removing the KCl prior to hydrolysis leads to bulk mesostructured Mo-TMS1 with no macroscopic order. The influence of salts on the formation of mesoporous silicate macrotubules has been studied recently.[24]

Attempts to remove surfactant either by acid treatment or ozone treatment led to formation of layered and amorphous materials, respectively. In an attempt to improve the structural strength of the material so that it would retain its structure on template removal, we subjected the bronze Mo-TMS1 to hydrothermal treatment in a sealed tube at 150 °C for ten days. Surprisingly, both the material and the supernatant had turned deep blue in color, a common hue for mixed oxidation state Mo oxides. The XRD pattern of this new molybdenum blue (Figure 1 B) showed that the material had converted into a lamellar structure with major peak at about 30 and 26 Å. Lower angle peaks with d values ranging from 15 to 6 Å were also observed, indicative that the walls or lamellae of the material had crystallized. The high-angle diffraction pattern revealed a series of peaks which can be indexed to a single-phase MoO_2 (Tugarinovite) that has a monoclinic structure (space group $P2_1/c$; $a = 5.608$, $b = 4.859$, $c = 5.537$ Å, $\beta = 119.37°$). This is indicative of crystallization of the walls of the bronze mesostructure. Highly crystallized walls have only been observed once in a mesoporous material.[8] The elemental analysis of this material showed that the stoichiometry of

  1433-7851/99/3810-1473 $ 17.50+.50/0

the molybdenum blue had not changed from the bronze. The XPS $3d_{5/2,3/2}$ emission (Figure 2) indicates that the surface oxidation state was modified with a distinct emission around 229.4 eV indicative of the enhanced presence of lower bound states for this material. On the other hand, interestingly, the Mo:O ratio (after removing the contribution of oxygen atoms related to C–O groups) was found to be again around 52%, in agreement with the presence of MoO_2. This is consistent with past work on mixed oxidation state molybdenum oxide clusters in which XPS studies revealed a mixture of Mo^{IV} and Mo^{VI}.[20] The valence spectra (Figure 2 inset) reveal that this mesostructure is a much better conductor than the bronze sample with practically no gap between the valence band and the Fermi level. This is comparable to that of MnO_2, which is nearly metallic in nature. The conductivity of this sample was $6.3 \times 10^{-7}\ \Omega\,cm^{-1}$, which is similar to the values previously reported for mesoporous Mn oxide.[8] Part of this conductivity, which should be even higher due to the position of the Fermi level in respect to the valence band, can be explained by the nanocrystalline nature of the material. Because the average grain size is on the order of 15 Å, a large part of the conductivity will be dominated by the grain boundary contribution, which can decrease the conductivity by at least one or two orders of magnitude as compared to the coarse grain counterparts.

TEM images at low magnification showed regions of lamellar structure with approximately 3 nm between the layers (Figure 3c) as well as some regions in which the toroidal structures were maintained. Further magnification at the fringes of the porous regions revealed that the mesopores had undergone a phase change into discontinuous nanoparticles of roughly 15 Å in size (Figure 3d). These regions can be compared to mesostructured tungsten-based materials in which the walls of the mesostructure are constructed of well-defined, but isolated tungsten oxo clusters.[16] The presence of grains in the individual lamellae of the layered region could not be confirmed in this study. This suggests that there are two rivaling phase changes at work in this system. In the first, the walls of the hexagonal mesopores restructure into individual grains, hence imposing a new level of structure on the material while at the same time destroying the structural integrity of the walls. In the second, the mesopores undergo a collapse into a lamellar structure with no crystallinity in the oxide lamellae. Phase changes between lamellar, cubic, and hexagonal mesostructures are common. Further heating did little to alter the XRD pattern of the material. These materials provide insight into the thermal collapse of mesoporous metal oxides into bulk crystalline phases of the metal oxide, suggesting that crystallization of the walls in a mesostructure leads to grain formation and growth along with destruction of the porous matrix. This further suggests that in many cases it may not be possible to form mesoporous oxides in which the walls are crystalline, as in zeolites, since crystallization of the walls may lead to angstrom-level reordering of the material into a different structure.

In summary, the templating of molybdenum oxides under conditions favoring both rodlike micelle and vesicle or microbubble formation has led to mixed-valent conducting toroidal structures which display long- and short-range order on many levels of scale. While emulsions and microbubbles can lead to macroporous structures with applications as waveguides and ultralightweight materials, liquid crystal micelle templating can lead to structures with order on the nanometer scale. By controlling nucleation conditions and growth, hierarchical structures with order on both the macro- and mesoscale can be achieved. Treatment of these toroids with a TEM electron beam leads to a unique phase evolution to form larger toroids, while heating to 150 °C leads to reordering of the mesostructure and formation of a new lamellar phase and nanocrystalline molybdenum oxide. These phase changes are accompanied by a color change from brown to blue and a dramatic narrowing of the gap to the Fermi level. We anticipate that these materials may open the doorway to electronically active macro-mesostructures with applications in electronic materials or catalysis.

Experimental Section

Molybdenum pentachloride (5.0 g, 18.3 mmol) was treated with bis(trimethylsilyl)dodecylamine (3.0 g, 9.2 mmol) in dry dichloromethane (50 mL) for 2 h at ambient temperature. The solvent was then removed in vacuo and potassium ethoxide (6.14 g, 73.2 mmol) in ethanol (50 mL) was added with cooling. Water (100 mL) was added to this mixture, and the resulting brown liquid was allowed to sit at ambient temperature for 24 h and then heated to 90 °C for two weeks. The deep bronze precipitate was collected by filtration and washed with three portions of ethanol and water and then dried at 100 °C overnight. This as-synthesized mesostructured molybdenum oxide material exhibited a peak in the XRD pattern at $d = 32$ Å and showed a large proportion of toroidal regions by TEM. Heat treatment for ten days at 150 °C in a sealed tube resulted in formation of a blue material with a lamellar XRD pattern as well as high-angle peaks attributable to Tugarinovite. This material had very few toroidal regions.

Received: August 13, 1998
Revised version: January 7, 1999 [Z12284IE]
German version: *Angew. Chem.* **1999**, *111*, 1555–1559

Keywords: mesoporosity · molybdenum · semiconductors · template synthesis

[1] C. T. Kresge, M. E. Leonowicz, W. J. Roth, J. C. Vartulli, J. S. Beck, *Nature* **1992**, *359*, 710–714.
[2] D. M. Antonelli, J. Y. Ying, *Curr. Opin. Colloid Interface Sci.* **1996**, *1*, 523–529.
[3] D. M. Antonelli, J. Y. Ying, *Angew. Chem.* **1996**, *108*, 461–464; *Angew. Chem. Int. Ed. Engl.* **1996**, *35*, 426–430.
[4] D. Walsh, S. Mann, *Nature* **1995**, *377*, 320–323.
[5] A. Imhof, D. J. Pine, *Nature* **1997**, *389*, 948–951.
[6] S. Mann, G. A. Ozin, *Nature* **1996**, *382*, 313–318.
[7] H. Yang, N. Coombs, G. A. Ozin, *Nature* **1997**, *386*, 692–695.
[8] Z.-R. Tian, W. Tong, J.-Y. Wang, N.-G. Duan, V. V. Krishnan, S. L. Suib, *Science* **1997**, *276*, 926–929.
[9] D. M. Antonelli, A. Nakahira, J. Y. Ying, *Inorg. Chem.* **1996**, *35*, 3126–3136.
[10] D. M. Antonelli, J. Y. Ying, *Chem. Mater.* **1996**, *8*, 874–881.
[11] U. Ciesla, S. Schacht, G. D. Stucky, K. Unger, F. Schuth, *Angew. Chem.* **1996**, *108*, 596–600; *Angew. Chem. Int. Ed. Engl.* **1996**, *35*, 541–543.
[12] J. S. Reddy, A. Sayari, *Catal. Lett.* **1996**, *38*, 219–223.
[13] M. S. Wong, D. M. Antonelli, J. Y. Ying, *Nanostruct. Mater.* **1997**, *9*, 165–168.
[14] D. M. Antonelli, J. Y. Ying, *Angew. Chem.* **1995**, *107*, 2202–2206; *Angew. Chem. Int. Ed. Engl.* **1995**, *34*, 2014–2017.
[15] P. Liu, J. Liu, A. Sayari, *Chem. Commun.* **1997**, 577–578.
[16] Q. Huo, D. I. Margolese, U. Ciesla, P. Feng, T. E. Gier, P. Sieger, R. Leon, P. M. Petroff, F. Schüth, G. Stucky, *Nature* **1994**, *368*, 317–320.

  1433-7851/99/3810-1474 $ 17.50+.50/0

[17] P. T. Tanev, M. Chibwe, T. J. Pinnavaia, *Nature* **1994**, *368*, 321 – 323.
[18] *Practical surface analysis: Vol. 1: Auger and X-ray photoelectron spectroscopy* (Eds.: D. Briggs, M. P. Seah), 2nd ed., Wiley, London, **1990**.
[19] S. O. Grim, L. J. Matienzo, *Inorg. Chem.* **1975**, *14*, 1014 – 1018.
[20] G. A. Ozin, S. Özkar, R. A. Prokopowicz, *Acc. Chem. Res.* **1992**, *25*, 553 – 560.
[21] Samples were prepared by grinding in a mortar and pestel in acetone and depositing on a slide. Reflectance mode spectra were run on an Ocean Optics S-2000 UV/Vis spectrometer. The band gap was calculated from the powder UV/Vis spectra as described in A. R. West, *Solid State Chemistry and its Applications*, Wiley, New York, **1984**, pp. 75 – 78.
[22] G. A. Ozin, *Acc. Chem. Res.* **1997**, *30*, 17 – 27.
[23] S. Oliver, A. Kuperman, N. Coombs, A. Lough, G. A. Ozin, *Nature* **1995**, *378*, 47 – 50.
[24] H.-P. Lin, S. Cheng, C.-Y. Mou, *Chem. Mater.* **1998**, *10*, 581 – 589.

$Ni(tpt)(NO_3)_2$—A Three-Dimensional Network with the Exceptional (12,3) Topology: A Self-Entangled Single Net**

Brendan F. Abrahams, Stuart R. Batten, Martin J. Grannas, Hasan Hamit, Bernard F. Hoskins, and Richard Robson*

In Memory of Dr. George Winter

Extended framework solids are currently of considerable interest and importance because of the scope they offer for the generation by design of new materials with a range of potentially useful properties.[1] A valuable conceptual approach to building and describing extended frameworks, in particular those involving interpenetration,[2] is based on the idea of a net, a valuable catalogue of which has been provided by Wells.[3]

Connecting ligands providing two or more bidentate metal-binding sites that are now starting to be explored,[4] are particularly appealing as building blocks for coordination polymers because they promise robust networks with good electronic communication between metal centers. When an octahedral metal center takes on three ligands of this type the metal center itself adopts the role of 3-connecting node giving access to a range of still little known 3-connecting nets. We suspect that many examples of 3-connected nets will appear in the near future. The symbol $(n,3)$ can be used to characterize the topologies of nets in which all nodes are 3-connecting and where the shortest circuits involving all three different pairs of connections radiating from each node are n-gons. An interesting question that arises when one considers the set of $(n,3)$ nets is "what is the largest possible value for n?"—or, in other words "what is the three-dimensional (3D) 3-connected net whose shortest circuits are as large as possible?". The (12,3) net is the one with the largest value of n considered by Wells.[1, 5] What we describe here is, to the best of our knowledge, the first real chemical example of a (12,3) net.

A representation of a (12,3) net with planar nodes is shown in Figure 1. The net, which is intrinsically chiral, can be visualized in terms of "double" sixfold helices, all of the same handedness and all parallel, connected together by links that are perpendicular to the helical axis. The extension of the (12,3) net in the direction of the helical axis is dictated by the angle at each node internal to the helix which can, in principle, take any value from 120° (regular trigonal nodes) to 180° (T-shaped nodes)—the larger this angle, the greater the pitch of the helices and the more extended in the direction of the helical axis does the structure become.

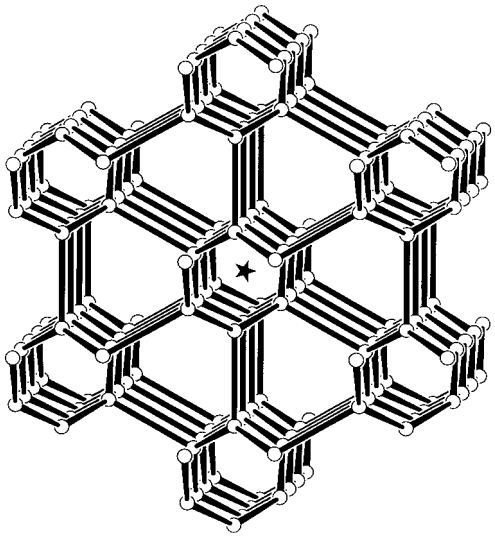

Figure 1. Representation of the (12,3) net in which all nodes are planar and equivalent. One sixfold double helix is highlighted with a star for ease of identification.

Whilst neither strictly trigonal nodes alone nor strictly T-shaped nodes alone can be used to generate the (12,3) net, it can be constructed in a completely strain-free manner from alternating T and trigonal nodes. This is precisely what we observe, as described below, in the structure of the crystalline coordination polymer[6] obtained from nickel nitrate and the trigonal 3-connecting ligand tri-4-pyridyl-1,3,5-triazine (tpt; **1**). This geometrically simple ligand has already afforded a> wide variety of unusual and symmetrical 3D coordination networks.[7] The crystal consists of a well-defined coordination polymer framework with the (12,3) topology containing equal numbers of tpt and Ni^{2+} centers. Disordered solvent occupies the chiral channels running parallel with the helical axes. The essence of the connectivity of the network is

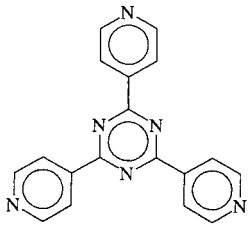

1

[*] Dr. R. Robson, Dr. B. F. Abrahams, Dr. S. R. Batten, Dr. M. J. Grannas, H. Hamit, Dr. B. F. Hoskins
School of Chemistry, University of Melbourne
Parkville, Victoria 3052 (Australia)
Fax: (+61) 3-9347-5180
E-mail: r.robson@chemistry.unimelb.edu.au

[**] The authors gratefully acknowledge support from the Australian Research Council.

  1433-7851/99/3810-1475 $ 17.50+.50/0